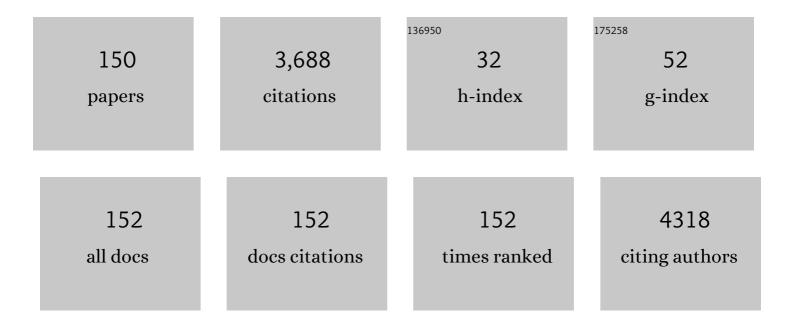
Shuang-Peng Wang

List of Publications by Year in descending order

Source: https://exaly.com/author-pdf/1659955/publications.pdf Version: 2024-02-01



#	Article	IF	CITATIONS
1	High gain Ga_2O_3 solar-blind photodetectors realized via a carrier multiplication process. Optics Express. 2015. 23. 13554 <mml:math <br="" xmlns:mml="http://www.w3.org/1998/Math/MathML">display="inline"><mml:mi>p</mml:mi></mml:math> -Type Conductivity in N-Doped ZnO: The Role of	3.4	153
2	the <mml:math <br="" xmlns:mml="http://www.w3.org/1998/Math/MathML">display="inline"> <mml:msub> <mml:mi mathvariant="normal">N <mml:mi>Zn</mml:mi> V <mml:mi> V</mml:mi> <mml:mi> V</mml:mi> <mml:mi> </mml:mi> <td>7.8</td><td>143</td></mml:mi </mml:msub></mml:math>	7.8	143
3	mathyariant – "normal" mathyariant – "normal" Self-powered spectrum-selective photodetectors fabricated from n-ZnO/p-NiO core–shell nanowire arrays. Journal of Materials Chemistry C, 2013, 1, 4445.	5.5	134
4	3D heterostructured pure and N-Doped Ni3S2/VS2 nanosheets for high efficient overall water splitting. Electrochimica Acta, 2018, 269, 55-61.	5.2	132
5	Development of Electrocatalysts for Efficient Nitrogen Reduction Reaction under Ambient Condition. Advanced Functional Materials, 2021, 31, 2008983.	14.9	124
6	Phosphorescent Carbon-Nanodots-Assisted Förster Resonant Energy Transfer for Achieving Red Afterglow in an Aqueous Solution. ACS Nano, 2021, 15, 16242-16254.	14.6	94
7	Multiâ€Phase Heterostructure of CoNiP/Co <i>_x</i> P for Enhanced Hydrogen Evolution Under Alkaline and Seawater Conditions by Promoting H ₂ O Dissociation. Small, 2021, 17, e2007557.	10.0	83
8	Two-dimensional materials as novel co-catalysts for efficient solar-driven hydrogen production. Journal of Materials Chemistry A, 2020, 8, 23202-23230.	10.3	81
9	Remarkable synergistic effect in cobalt-iron nitride/alloy nanosheets for robust electrochemical water splitting. Journal of Energy Chemistry, 2022, 65, 405-414.	12.9	81
10	Emerging core–shell nanostructures for surface-enhanced Raman scattering (SERS) detection of pesticide residues. Chemical Engineering Journal, 2021, 424, 130323.	12.7	72
11	Development of Perovskite Oxideâ€Based Electrocatalysts for Oxygen Evolution Reaction. Small, 2021, 17, e2101605.	10.0	71
12	Polyoxometalateâ€Derived Hexagonal Molybdenum Nitrides (MXenes) Supported by Boron, Nitrogen Codoped Carbon Nanotubes for Efficient Electrochemical Hydrogen Evolution from Seawater. Advanced Functional Materials, 2019, 29, 1805893.	14.9	69
13	Photoconductive gain in solar-blind ultraviolet photodetector based on Mg0.52Zn0.48O thin film. Applied Physics Letters, 2011, 99, 242105.	3.3	68
14	Electrically pumped random lasers fabricated from ZnO nanowire arrays. Nanoscale, 2012, 4, 2843.	5.6	66
15	2D materials: Excellent substrates for surface-enhanced Raman scattering (SERS) in chemical sensing and biosensing. TrAC - Trends in Analytical Chemistry, 2020, 130, 115983.	11.4	66
16	High-Brightness and Color-Tunable FAPbBr ₃ Perovskite Nanocrystals 2.0 Enable Ultrapure Green Luminescence for Achieving Recommendation 2020 Displays. ACS Applied Materials & Interfaces, 2020, 12, 2835-2841.	8.0	61
17	Surface mediated ligands addressing bottleneck of room-temperature synthesized inorganic perovskite nanocrystals toward efficient light-emitting diodes. Nano Energy, 2020, 70, 104467.	16.0	56
18	Theoretical evidence of the spin–valley coupling and valley polarization in two-dimensional MoSi ₂ X ₄ (X = N, P, and As). Physical Chemistry Chemical Physics, 2021, 23, 3144-3151.	2.8	53

#	Article	IF	CITATIONS
19	Fast Response Organic Tandem Photodetector for Visible and Nearâ€Infrared Digital Optical Communications. Small, 2021, 17, e2101316.	10.0	49
20	ZnO-based ultraviolet avalanche photodetectors. Journal Physics D: Applied Physics, 2013, 46, 305105.	2.8	48
21	Fluorometric determination of pesticides and organophosphates using nanoceria as a phosphatase mimic and an inner filter effect on carbon nanodots. Mikrochimica Acta, 2019, 186, 66.	5.0	47
22	Single-step synthesis of polychromatic carbon quantum dots for macroscopic detection of Hg2+. Ecotoxicology and Environmental Safety, 2020, 190, 110141.	6.0	46
23	Enhanced Responsivity of Highly Spectrum-Selective Ultraviolet Photodetectors. Journal of Physical Chemistry C, 2012, 116, 1350-1353.	3.1	41
24	Stable and Efficient Blueâ€Emitting CsPbBr ₃ Nanoplatelets with Potassium Bromide Surface Passivation. Small, 2021, 17, e2101359.	10.0	41
25	Ultraviolet photodetectors fabricated from ZnO p–i–n homojunction structures. Materials Chemistry and Physics, 2011, 129, 27-29.	4.0	40
26	In-situ generation of Ni-CoOOH through deep reconstruction for durable alkaline water electrolysis. Chemical Engineering Journal, 2022, 443, 136432.	12.7	38
27	Anodized Steel: The Most Promising Bifunctional Electrocatalyst for Alkaline Water Electrolysis in Industry. Advanced Functional Materials, 2022, 32, .	14.9	37
28	Fluorescent and visual detection of methyl-paraoxon by using boron-and nitrogen-doped carbon dots. Microchemical Journal, 2020, 154, 104547.	4.5	36
29	Aligned Millineedle Arrays for Solar Power Seawater Desalination with Siteâ€Specific Salt Formation. Small, 2021, 17, e2101487.	10.0	36
30	Piezophototronicâ€Effectâ€Enhanced Electrically Pumped Lasing. Advanced Materials, 2017, 29, 1602832.	21.0	35
31	Theoretical Screening of Single Atoms Supported on Two-Dimensional Nb ₂ CN ₂ for Nitrogen Fixation. ACS Applied Nano Materials, 2020, 3, 11274-11281.	5.0	34
32	Pressure and temperature-dependent Raman spectra of MoS2 film. Applied Physics Letters, 2016, 109, .	3.3	33
33	Ultrafine WC _{1–<i>x</i>} Nanocrystals: An Efficient Cocatalyst for the Significant Enhancement of Photocatalytic Hydrogen Evolution on g-C ₃ N ₄ . Journal of Physical Chemistry C, 2019, 123, 26136-26144.	3.1	33
34	High-Efficiency and Stable Inverted Planar Perovskite Solar Cells with Pulsed Laser Deposited Cu-Doped NiO _{<i>x</i>} Hole-Transport Layers. ACS Applied Materials & Interfaces, 2020, 12, 50684-50691.	8.0	33
35	Vertically-aligned 1T/2H-MS2 (MÂ=ÂMo, W) nanosheets for surface-enhanced Raman scattering with long-term stability and large-scale uniformity. Applied Surface Science, 2020, 527, 146769.	6.1	33
36	Enhanced solar-blind responsivity of photodetectors based on cubic MgZnO films via gallium doping. Optics Express, 2014, 22, 246.	3.4	32

#	Article	IF	CITATIONS
37	Surface polarity control in ZnO films deposited by pulsed laser deposition. Applied Surface Science, 2019, 483, 1129-1135.	6.1	32
38	Combined Experimental and Theoretical Assessment of WX _{<i>y</i>} (X = C, N, S, P) for Hydrogen Evolution Reaction. ACS Applied Energy Materials, 2020, 3, 1082-1088.	5.1	32
39	Close-loop recycling of perovskite solar cells through dissolution-recrystallization of perovskite by butylamine. Cell Reports Physical Science, 2021, 2, 100341.	5.6	32
40	Corrosion engineering boosting bulk Fe50Mn30Co10Cr10 high-entropy alloy as high-efficient alkaline oxygen evolution reaction electrocatalyst. Journal of Materials Science and Technology, 2022, 109, 267-275.	10.7	32
41	Degradation of quantum dot light emitting diodes, the case under a low driving level. Journal of Materials Chemistry C, 2020, 8, 2014-2018.	5.5	31
42	Pure ultraviolet emission from ZnO nanowire-based p-n heterostructures. Optics Letters, 2014, 39, 422.	3.3	30
43	Influence of Shell Thickness on the Performance of NiO-Based All-Inorganic Quantum Dot Light-Emitting Diodes. ACS Applied Materials & Interfaces, 2018, 10, 14894-14900.	8.0	30
44	Electrocatalytic Hydrogen Production: Polyoxometalateâ€Derived Hexagonal Molybdenum Nitrides (MXenes) Supported by Boron, Nitrogen Codoped Carbon Nanotubes for Efficient Electrochemical Hydrogen Evolution from Seawater (Adv. Funct. Mater. 8/2019). Advanced Functional Materials, 2019, 29, 1970046.	14.9	28
45	Electrical and optical properties of ZnO films grown by molecular beam epitaxy. Applied Surface Science, 2009, 255, 4913-4915.	6.1	26
46	Influence of Zn/O ratio on structural, electrical and optical properties of ZnO thin films fabricated by plasma-assisted molecular beam epitaxy. Journal of Alloys and Compounds, 2010, 503, 155-158.	5.5	26
47	Mott-type MgxZn1-xO-based visible-blind ultraviolet photodetectors with active anti-reflection layer. Applied Physics Letters, 2013, 102, 231122.	3.3	26
48	Electrically Driven Single Microwire-Based Heterojuction Light-Emitting Devices. ACS Photonics, 2017, 4, 1286-1291.	6.6	26
49	Tailoring the Photoluminescence Excitation Dependence of the Carbon Dots via an Alkali Treatment. Journal of Physical Chemistry Letters, 2019, 10, 4596-4602.	4.6	26
50	3D V–Ni3S2@CoFe-LDH core-shell electrocatalysts for efficient water oxidation. International Journal of Hydrogen Energy, 2021, 46, 39636-39644.	7.1	26
51	N and V Coincorporated Ni Nanosheets for Enhanced Hydrogen Evolution Reaction. ACS Sustainable Chemistry and Engineering, 2018, 6, 16525-16531.	6.7	25
52	Lithography-Free Formation of Controllable Microdomes via Droplet Templates for Robust, Ultrasensitive, and Flexible Pressure Sensors. ACS Applied Nano Materials, 2019, 2, 7178-7187.	5.0	25
53	Thermal stability and photoluminescence of Mn2+ activated green-emitting feldspar phosphor SrAl2Si2O8: Mn2+ for wide gamut w-LED backlight. Optical Materials, 2020, 99, 109535.	3.6	25
54	Mo incorporated Ni nanosheet as high-efficiency co-catalyst for enhancing the photocatalytic hydrogen production of g-C3N4. International Journal of Hydrogen Energy, 2020, 45, 18912-18921.	7.1	25

#	Article	IF	CITATIONS
55	Effect of compressive stress on stability of N-doped p-type ZnO. Applied Physics Letters, 2011, 99, 091908.	3.3	24
56	Enhanced Responsivity of Photodetectors Realized via Impact Ionization. Sensors, 2012, 12, 1280-1287.	3.8	24
57	Enhancement of Visibleâ€Light Photocatalytic Hydrogen Production by CeCO ₃ OH in g ₃ N ₄ /CeO ₂ System. ChemCatChem, 2019, 11, 1069-1075.	3.7	24
58	Unravelling the Reaction Mechanisms of N ₂ Fixation on Molybdenum Nitride: A Full DFT Study from the Pristine Surface to Heteroatom Anchoring. ChemSusChem, 2021, 14, 3257-3266.	6.8	22
59	Suppression of coffee-ring effect <i>via</i> periodic oscillation of substrate for ultra-sensitive enrichment towards surface-enhanced Raman scattering. Nanoscale, 2019, 11, 20534-20545.	5.6	21
60	Shape-control growth of 2D-In ₂ Se ₃ with out-of-plane ferroelectricity by chemical vapor deposition. Nanoscale, 2020, 12, 20189-20201.	5.6	21
61	Intense emission from ZnO nanocolumn Schottky diodes. Nanoscale, 2013, 5, 7746.	5.6	20
62	Optoelectronic Modulation of Undoped NiO _{<i>x</i>} Films for Inverted Perovskite Solar Cells via Intrinsic Defect Regulation. ACS Applied Energy Materials, 2020, 3, 9732-9741.	5.1	20
63	Design of phosphorus-functionalized MXenes for highly efficient hydrogen evolution reaction. Journal of Materials Chemistry A, 2021, 9, 597-606.	10.3	20
64	Single stain hyperspectral imaging for accurate fungal pathogens identification and quantification. Nano Research, 2022, 15, 6399-6406.	10.4	20
65	On the origin of intrinsic donors in ZnO. Applied Surface Science, 2010, 256, 3390-3393.	6.1	19
66	Stable UV-Pumped White Light-Emitting Diodes Based on Anthracene-Coated CsCu ₂ 1 ₃ . Journal of Physical Chemistry C, 2021, 125, 13076-13083.	3.1	19
67	Graphene induced high-Q hybridized plasmonic whispering gallery mode microcavities. Optics Express, 2014, 22, 23836.	3.4	18
68	Numerical investigation of the effect of laser shock peening parameters on the residual stress and deformation response of 7075 aluminum alloy. Optik, 2021, 243, 167446.	2.9	18
69	A facile route to arsenic-doped p-type ZnO films. Journal of Crystal Growth, 2009, 311, 3577-3580.	1.5	17
70	Band offset and an ultra-fast response UV-VIS photodetector in γ-In ₂ Se ₃ /p-Si heterojunction heterostructures. RSC Advances, 2018, 8, 29555-29561.	3.6	17
71	Waved 2D Transition-Metal Disulfides for Nanodevices and Catalysis: A First-Principle Study. ACS Applied Nano Materials, 2020, 3, 2804-2812.	5.0	17
72	Co3Mo3N nanosheets arrays on nickel foam as highly efficient bifunctional electrocatalysts for overall urea electrolysis. International Journal of Hydrogen Energy, 2022, 47, 11447-11455.	7.1	17

#	Article	IF	CITATIONS
73	Ultra-low threshold avalanche gain from solar-blind photodetector based on graded-band-gap-cubic-MgZnO. Optics Express, 2015, 23, 32329.	3.4	16
74	Networkâ€Like Ni _{1â^'x} Mo _x Nanosheets: Multiâ€Functional Electrodes for Overall Water Splitting and Supercapacitor. ChemElectroChem, 2019, 6, 1338-1343.	3.4	16
75	Aluminum-Based Surface Polymerization on Carbon Dots with Aggregation-Enhanced Luminescence. Journal of Physical Chemistry Letters, 2021, 12, 4530-4536.	4.6	16
76	Black-colored ZnO nanowires with enhanced photocatalytic hydrogen evolution. Nanotechnology, 2016, 27, 22LT01.	2.6	15
77	A one-dimensional random laser based on artificial high-index contrast scatterers. Nanoscale, 2017, 9, 6959-6964.	5.6	15
78	Dialkylamines Driven Two-Step Recovery of NiO _{<i>x</i>} /ITO Substrates for High-Reproducibility Recycling of Perovskite Solar Cells. Journal of Physical Chemistry Letters, 2021, 12, 4735-4741.	4.6	15
79	Co ₂ N _{0.67} /MoO ₂ Heterostructure as High-Efficiency Electrocatalysts for the Hydrogen Evolution Reaction. ACS Applied Energy Materials, 2022, 5, 440-448.	5.1	15
80	Intense electroluminescence from ZnO nanowires. Journal of Materials Chemistry C, 2015, 3, 5292-5296.	5.5	14
81	High transmittance Er-doped ZnO thin films as electrodes for organic light-emitting diodes. Applied Physics Letters, 2019, 115, .	3.3	14
82	Robust Ultralong Lead Halide Perovskite Microwire Lasers. ACS Applied Materials & Interfaces, 2021, 13, 38458-38466.	8.0	14
83	Waferâ€6cale 2Hâ€MoS ₂ Monolayer for High Surfaceâ€enhanced Raman Scattering Performance: Chargeâ€Transfer Coupled with Molecule Resonance. Advanced Materials Technologies, 2022, 7, .	5.8	14
84	Random lasing realized in n-ZnO/p-MgZnO core–shell nanowire heterostructures. CrystEngComm, 2015, 17, 3917-3922.	2.6	13
85	Substrate strain engineering: an efficient strategy to enhance the catalytic activity of SACs on waved graphene for e-NRR. Sustainable Energy and Fuels, 2020, 4, 3773-3779.	4.9	13
86	Aliphatic Group-Tethered Iridium Complex as a Theranostic Agent against Malignant Melanoma Metastasis. ACS Applied Bio Materials, 2020, 3, 2017-2027.	4.6	13
87	Enhanced p-Type Conductivity of NiO _{<i>x</i>} Films with Divalent Cd Ion Doping for Efficient Inverted Perovskite Solar Cells. ACS Applied Materials & Interfaces, 2022, 14, 17434-17443.	8.0	13
88	Phosphor-converted light-emitting diode based on ZnO-based heterojunction. Journal of Luminescence, 2010, 130, 2215-2217.	3.1	12
89	Lowâ€Threshold Whisperingâ€Gallery Mode Upconversion Lasing via Simultaneous Sixâ€Photon Absorption. Advanced Optical Materials, 2018, 6, 1800407.	7.3	12
90	Homogeneous Core/Shell NiMoO4@NiMoO4 and Activated Carbon for High Performance Asymmetric Supercapacitor. Nanomaterials, 2019, 9, 1033.	4.1	12

6

#	Article	IF	CITATIONS
91	Fabry-Perot resonance enhanced electrically pumped random lasing from ZnO films. Applied Physics Letters, 2015, 107, .	3.3	11
92	Transparent ultraviolet photovoltaic cells. Optics Letters, 2016, 41, 685.	3.3	11
93	Investigation on the role of amines in the liquefaction and recrystallization process of MAPbI ₃ perovskite. Journal of Materials Chemistry A, 2020, 8, 13585-13593.	10.3	11
94	1T‴Transition-Metal Dichalcogenides: Strong Bulk Photovoltaic Effect for Enhanced Solar-Power Harvesting. Journal of Physical Chemistry C, 2020, 124, 11221-11228.	3.1	11
95	In situ surface reconstruction on LaCoO3â^î´ leads to enhanced hydrogen evolution reaction. Journal of Alloys and Compounds, 2022, 891, 161754.	5.5	11
96	A route to single-crystalline ZnO films with low residual electron concentration. Journal of Crystal Growth, 2010, 312, 2861-2864.	1.5	10
97	Degenerated MgZnO films obtained by excessive zinc. Journal of Crystal Growth, 2012, 347, 95-98.	1.5	10
98	Bias-Polarity Dependent Ultraviolet/Visible Switchable Light-Emitting Devices. ACS Applied Materials & Interfaces, 2014, 6, 8257-8262.	8.0	10
99	A simple method for the preparation of multi-color carbon quantum dots by using reversible regulatory color transformation. Mikrochimica Acta, 2019, 186, 612.	5.0	10
100	A new fluorescent technique for pesticide detection by using metal coordination polymer and nanozyme. Chinese Medicine, 2020, 15, 22.	4.0	10
101	Solvent Effects on the Interface and Film Integrity of Solution-Processed ZnO Electron Transfer Layers for Quantum Dot Light-Emitting Diodes. ACS Applied Electronic Materials, 2020, 2, 1074-1080.	4.3	10
102	Quaternary-metal phosphide as electrocatalyst for efficient hydrogen evolution reaction in alkaline solution. International Journal of Hydrogen Energy, 2021, 46, 18878-18886.	7.1	10
103	Development of Perovskite Oxideâ€Based Electrocatalysts for Oxygen Evolution Reaction (Small) Tj ETQq1 1 0.78	84314 rgB 10.0 rgB	T /Overlock
104	Surface Periodic Nanostructure of <1>p-GaSb Irradiated by Femtosecond Laser and Optical Properties Research. Nanoscience and Nanotechnology Letters, 2015, 7, 1-5.	0.4	9
105	Ultraviolet emissions excited by accelerated electrons. Optics Letters, 2012, 37, 1568.	3.3	8
106	Low-Cost Flexible ZnO Microwires Array Ultraviolet Photodetector Embedded in PAVL Substrate. Nanoscale Research Letters, 2018, 13, 277.	5.7	8
107	IP and OOP ferroelectricity in hexagonal γ-In2Se3 nanoflakes grown by chemical vapor deposition. Journal of Alloys and Compounds, 2021, 870, 159344.	5.5	8
108	The catalyst-free growth of layer-structured CuInSe ₂ /β-In ₂ Se ₃ microwires for ultrasensitive self-powered photodetectors based on a lateral p–n junction. Journal of Materials Chemistry C, 2021, 9, 9484-9491.	5.5	8

#	Article	IF	CITATIONS
109	Insightful view on the active sites of Ni/NixP for hydrogen evolution reaction. Applied Materials Today, 2022, 26, 101343.	4.3	8
110	On the accurate characterization of quantum-dot light-emitting diodes for display applications. Npj Flexible Electronics, 2022, 6, .	10.7	8
111	Conduction band discontinuity and carrier multiplication at the Mg _x Zn _{1â^'x} O/Mg _y Zn _{1â^'y} O interface. RSC Advances, 2016, 6, 34955-34958.	3.6	7
112	Freestanding CH ₃ NH ₃ PbBr ₃ single-crystal microwires for optoelectronic applications synthesized with a predefined lattice framework. Journal of Materials Chemistry C, 2021, 9, 4771-4781.	5.5	7
113	Multichannel Generations of Orbital Angular Momentum Modes with Onâ€Demand Characteristics on a Chip. Advanced Optical Materials, 2021, 9, 2101308.	7.3	7
114	Investigation by nanosecond fiber laser for hybrid color marking and its potential application. Optics and Laser Technology, 2022, 147, 107553.	4.6	7
115	Realization of integrative hierarchy by in-situ solidification of â€̃semi-cured' microcilia array in candle flame for robust and flexible superhydrophobicity. Chemical Engineering Journal, 2022, 432, 134400.	12.7	6
116	Advances in oxide semiconductors for surface enhanced Raman scattering. Applied Materials Today, 2022, 29, 101563.	4.3	6
117	Degenerate layer at ZnO/sapphire interface. Journal Physics D: Applied Physics, 2009, 42, 195403.	2.8	5
118	Observation and Suppression of Stacking Interface States in Sandwich-Structured Quantum Dot Light-Emitting Diodes. ACS Applied Materials & Interfaces, 2021, 13, 56630-56637.	8.0	5
119	Control of N/N2 species ratio in NO plasma for p-type doping of ZnO. Journal of Applied Physics, 2011, 110, .	2.5	4
120	Flexible ultrahigh <i>Q</i> -factor bottle-like microcavity laser. Journal Physics D: Applied Physics, 2018, 51, 065107.	2.8	4
121	Controlled compensation via non-equilibrium electrons in ZnO. Scientific Reports, 2018, 8, 17020.	3.3	3
122	Synthesis of Core‧hell Au@TiO 2 @C Nanoparticles and Their Photocatalytic Properties for the Degradation of Rhodamine B Under Simulated‧olar Light. ChemistrySelect, 2020, 5, 10055-10059.	1.5	3
123	Activated Triplet Exciton Release for Highly Efficient Room-Temperature Phosphorescence Based on S,N-Doped Polymeric Carbon Nitride. Journal of Physical Chemistry Letters, 2022, 13, 726-732.	4.6	3
124	Mixed Two-Dimensional Organic-Inorganic Halide Perovskites for Highly Efficient and Stable Photovoltaic Application. Molecules, 2019, 24, 2144.	3.8	2
125	Giant moiré trapping of excitons in twisted hBN. Optics Express, 2022, 30, 10596.	3.4	2
126	Directed exfoliating and ordered stacking of transition-metal-dichalcogenides. Nanoscale, 2022, 14, 7484-7492.	5.6	2

#	Article	IF	CITATIONS
127	Structural Engineering of Ultrathin, Lightweight, and Bendable Electrodes Based on a Nanowire Network Current Collector Enables Flexible Energy-Storage Devices. ACS Applied Energy Materials, 2022, 5, 5785-5796.	5.1	2
128	The Electrical Characteristics of GaAs-MgO Interfaces of GaAs MIS Schottky Diodes. Advanced Materials Research, 0, 1118, 270-275.	0.3	1
129	Photoluminescence Analysis of the Ternary Alloy GaAsSb Sulfur Passivation. , 2015, , .		1
130	Enhancing ultraviolet photoresponsivity of an oversized Sn-doped ZnO microwire based photodetector. Journal of Materials Science: Materials in Electronics, 2019, 30, 518-524.	2.2	1
131	Synthesis and Characterization of ZnO/Ag-Doped ZnO Core–Shell Nanowires. Nanoscience and Nanotechnology Letters, 2015, 7, 643-647.	0.4	1
132	Electrical Properties of ZnO Thin Films Growth Under Different Conditions. Chinese Journal of Luminescence, 2013, 34, 1430-1434.	0.5	1
133	Smooth Surface Morphology of ZnO Thin Films on Sapphire at Low Temperature. Chinese Journal of Luminescence, 2014, 35, 542-547.	0.5	1
134	Effect of Boron on Nitrogen Doped p-type ZnO Thin Films. Chinese Journal of Luminescence, 2014, 35, 795-799.	0.5	1
135	Efficiency Improvement of Quantum Dot Light-Emitting Diodes via Thermal Damage Suppression with HATCN. ACS Applied Materials & Interfaces, 2021, 13, 49058-49065.	8.0	1
136	One-step synthesized single component white emitting carbon microspheres for lighting. Journal of Luminescence, 2022, 242, 118606.	3.1	1
137	Ultraviolet emissions realized in ZnO via an avalanche multiplication process. Chinese Physics B, 2013, 22, 077307.	1.4	Ο
138	Progress on Preparation of InAs Nanowires by Molecular Beam Epitaxy. Materials Science Forum, 0, 852, 349-355.	0.3	0
139	Enhanced Secondâ€Harmonic Generation in a Single Microwire Based on Localized Surface Plasmon. Physica Status Solidi (B): Basic Research, 2019, 256, 1900075.	1.5	Ο
140	First-principles study on electronic and optical properties of Mg-N dual-acceptor codoped CuAlO ₂ . Materials Research Express, 2021, 8, 015904.	1.6	0
141	Hybrid plasmonic leaky-mode lasing on subwavelength scale. Chinese Optics, 2021, 14, 397-408.	0.6	Ο
142	Decrease of Optimal Accelerating Voltage of ZnO-based Quantum Wells Pumped by Electron Beam. Chinese Journal of Luminescence, 2013, 34, 692-697.	0.5	0
143	Quantum-confined Stark Effects in Cathodoluminescence of ZnO/Zn0.85Mg0.15O Quantum Wells Pumped by Large Beam Current. Chinese Journal of Luminescence, 2013, 34, 1270-1274.	0.5	0
144	Improvement of Internal Quantum Efficiency of Asymmetric ZnO/ZnMgO Multi-quantum Wells. Chinese Journal of Luminescence, 2013, 34, 872-876.	0.5	0

#	Article	IF	CITATIONS
145	Controlled Growth of Pure Cubic Mg0.3Zn0.7O Thin Films on c-plane Sapphire by Introducing Graded Buffer Layer. Chinese Journal of Luminescence, 2014, 35, 1040-1045.	0.5	ο
146	Epitaxial (110)-oriented Cubic MgZnO Films on m-plane Sapphire for Solar-blind UV Photodetectors. Chinese Journal of Luminescence, 2014, 35, 678-683.	0.5	0
147	Cubic MgZnO Deep-ultraviolet Photodetector with High Responsivity. Chinese Journal of Luminescence, 2014, 35, 1291-1296.	0.5	0
148	p-type Doping of ZnOâ^¶N Thin Fims by Alternating The Growth Atmosphere. Chinese Journal of Luminescence, 2014, 35, 399-403.	0.5	0
149	Optical Properties of Arsenic-Doped MgZnO Films Treated by Thermal Annealing. Nanoscience and Nanotechnology Letters, 2015, 7, 817-821.	0.4	0
150	Effect of deposition temperature on the structural and surface properties of AlN by plasma enhanced atomic layer deposition. Hongwai Yu Jiguang Gongcheng/Infrared and Laser Engineering, 2016, 45, 0421001.	0.4	0